Proceedings of Global Power and Propulsion Society
ISSN-Nr: 2504-4400
GPPS Hong Kong 2023
October 17-19, 2023
www.gpps.global

GPPS-TC-2023-0269

Study on Combustion instability of Secondary Combustion in an Axial Staged Model Combustor

Bing Ge*
School of Mechanical Engineering, Shanghai Jiao Tong University
Gebing@sjtu.edu.cn
Shanghai, China

Yuliang Jia
Advanced Power Research Institute, Hangzhou Steam Turbine Co. LTD
Hangzhou, China

Yuze Li
School of Mechanical Engineering, Shanghai Jiao Tong University
Shanghai, China

Min Jin
School of Mechanical Engineering, Shanghai Jiao Tong University
Shanghai, China

Shusheng Zang
School of Mechanical Engineering, Shanghai Jiao Tong University
Shanghai, China

ABSTRACT

The experimental study is carried out to reveal the influence of the disturbance of main combustion air inlet on the axial staged combustion. The response of the combustion characteristics in the primary and secondary combustion chambers are obtained by acoustically forcing the inlet air to oscillate. The results indicate that the dominant frequency of combustion oscillation in the axial staged combustor is basically as the same as that of acoustic excitation. The pressure is more pronounced at the forced frequency of 270 Hz. Compared with the stable combustion state, the reburning flame is lifted and shrinks when the main air is oscillated. The spatial band area of the flame centroid fluctuations is transformed from the height (Y) direction to the streamwise (Z) direction. Combustion oscillation reduces the fluctuation range of reburning flame in the Y direction but expands in the Z direction. It is found that the dominant frequency of 201 Hz appears along in both Y and Z directions at the stable combustion status. In the case of forced oscillation, the dominant frequency of 270 Hz occurs along the Z and Y directions, and the amplitude of the original fluctuation of the reburning flame in the Z direction increases.

1. INTRODUCTION

The axial staged combustion has been proven to be an advanced combustion technology for reducing pollutant emissions [1-3]. Through the staged injection of fuel, the temperature of the combustion chamber is maintained at a low level, so that the NOx generation rate is greatly inhibited. Therefore, the axial staged combustion strategy shows great advantage in controlling NOx and CO emissions. This technology is mainly applied to high-grade gas turbines by GE [3,4], Kawasaki [5] and Ansaldo [6] to achieve higher efficiency and lower pollutant emissions [7] at the condition of high combustion temperature. In addition to emissions, the reburning flame structure is also the focus of axial staged combustion. Yi et al. [8] analyzed the mechanism by which spontaneous combustion of non-premixed jets in the mainstream controls flame initiation and stabilization. In the study performed by Roa et al. [9], it was found that the reburning flame is composed of two branches on the windward and the leeward sides respectively. The windward side flame is very unstable, and there will be three typical forms: complete flame attachment, unstable uplift, and blown away by the wind. Zheng [10] carried out numerical simulation on the reburning flame of axial staged combustion, and the results showed that the flame on the windward side presents distinct discontinuity, and the flame on the leeward side is continuously and stably attached to the reburning nozzle outlet.

However, since the lean premixed combustion is normally utilized for the primary combustion, it must consider the problem of combustion oscillation for the axial staged combustion. Ni et al. [11] proposed a self-excited combustion instability mechanism in the axial staged combustor, which involves the coupling between acoustic characteristics, autoignition time, flame velocity, fuel arrangement, and heat release intensity. Schulz et al. [12] analyzed the LES flame dynamics and concluded that due to the self-excited out-of-phase oscillation of the mixing temperature and axial velocity, the self-ignition length of the mixing section is strongly modulated, resulting in a strong position oscillation of the refiring zone.

At present, many studies have been carried out on the emission and the structure of the refiring flame, but there are relatively few studies on the combustion oscillation of the axial staged combustor, and the mechanism of the combustion oscillation is still unclear. In this work, disturbances are added to the main combustion air inlet by means of acoustic excitation, and the response of sound pressure fluctuations in the axial staged combustion chamber to the disturbance of the main combustion air inlet and the characteristics of the reburning flame are studied.

2. EXPERIMENTAL METHOD

Please follow the format above for the Title, header, paper number, author info, etc.

The combustion test system of the axially staged combustor is shown in Fig.1. It is mainly composed of the main combustion air supply system, the reburning air supply system, the fuel supply system, the axially staged combustor, the combustion test bench measurement system and other auxiliary systems. Among them, P1, P2 and P3 are respectively the main combustion air inlet of the combustion chamber, the sound pressure measurement points of the main combustion chamber and the secondary combustion chamber. A loudspeaker is provided upstream of the main combustion air inlet to provide sine wave acoustic excitation with a power of 300 W.

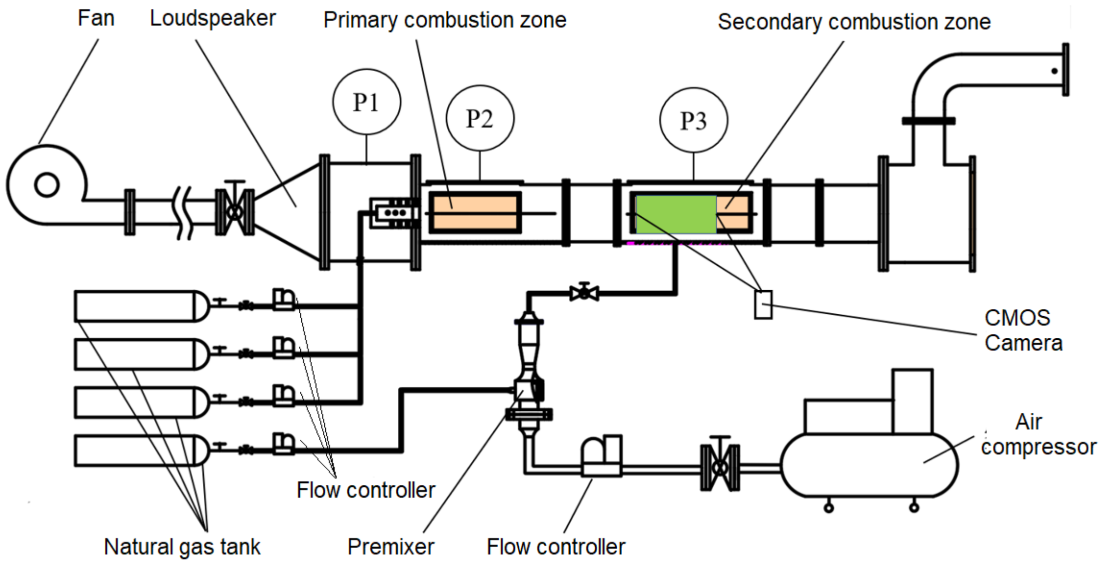

Fig.1 Axial staged combustor combustion test system

In this paper, the fuel is nature gas, and the main combustion premixed gas burns through the main combustion zone, and then enters the re-combustion zone after passing through the 116 mm steady flow transition zone. The cross-sectional size of the reburning zone is 144 mm*96 mm, and the inner diameter of the jet hole (D) is 12mm. The reburning premixed gas and the mainstream high-temperature flue gas are mixed and burned in the combustion zone. Figure 2 shows the model of the axial staged combustion chamber and defines the three-dimensional coordinates of the reburning region. The Z direction is the streamwise direction, the Y direction is the height direction, and the X direction is perpendicular to the view and inward. The coordinate origin is located at the center of the jet outlet circle.

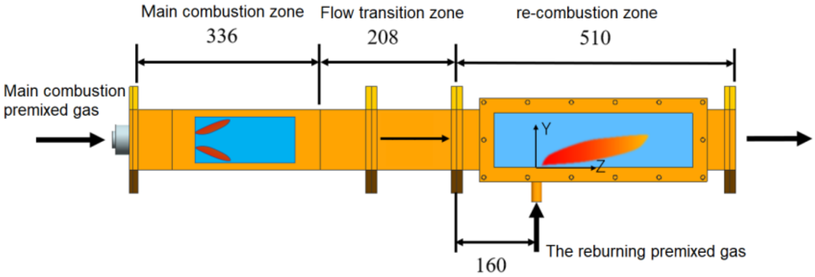

Fig.2 Axial staged combustion chamber

The photography of the reburning flame uses a high-resolution industrial camera Phantom VEO710, a high-speed camera with a resolution of 1080×800 pixels, and a maximum shooting frequency of 7400 Hz. The characteristic of methane/air reburning flame is studied by CH*-based self-luminescence test technique. In the mechanism of methane/air combustion reaction, CH* group is an important intermediate product in the combustion reaction, which can characterize the combustion reaction region, and its self-luminous emission wavelengths are 390 nm and 431 nm. In this experiment, a narrow-band filter with a wavelength of 432nm was used to capture the jet flames. The light transmittance of the used filter to the wavelength of 432±10 nm is above 90%, and the light transmittance of other wavelengths is lower than 1%. In order to measure the response of each area to the inlet air disturbance under the combustion oscillation of the axial staged combustion chamber, the microphone sensors (PCB 130F20) are used to measure the sound pressure at each measuring point of the combustion chamber, and the sound pressure sampling frequency is set to 2500 Hz. The measured sound pressure signal obtains frequency domain information through Fast Fourier Transform (FFT).

In this paper, the fuel/air equivalence ratio in the main combustion chamber and the reburning chamber is defined as follows:

$$\emptyset_m = \frac{m_{m,f}}{m_{m,a}} \times 17.16 \tag{1}$$

$$\emptyset_r = \frac{m_{r,f}}{m_{r,a}} \times 17.16 \tag{2}$$

Among them, $\emptyset_m$ and $\emptyset_r$ are the equivalence ratios for the main combustion chamber and the reburning chamber respectively. $m_{m,f}$ and $m_{r,f}$ are the fuel mass flow rate for two combustion chambers. $m_{m,a}$ and $m_{r,a}$ are air mass flow rates.

In the tests, the inlet air and fuel are gases at ambient temperature and pressure. The main combustion air mass flow rate is 114.6 g/s, the equivalence ratios for the main combustion and reburning is 0.53 and 0.8. Changing the main combustion air entrance sound excitation frequency changes the entrance disturbance. The specific test conditions are shown in Table 1.

Tab.1 Test conditions

Cases	$\emptyset_m$	$\emptyset_r$	Excitation frequency/Hz
1	0.53	0.80	0
2	0.53	0.80	110
3	0.53	0.80	190
4	0.53	0.80	270

3.Results and discussion

3.1 Acoustic pressure response of combustion chamber under forced oscillation

It is found that the main frequency of the oscillation in the combustion chamber is basically the same as the frequency of the acoustic excitation. In addition, compared with no reburning, the addition of reburning fuel has little effect on the combustion oscillation of the combustion chamber, but the response of the combustion chamber will be significantly different with the addition of different acoustic excitation frequencies.

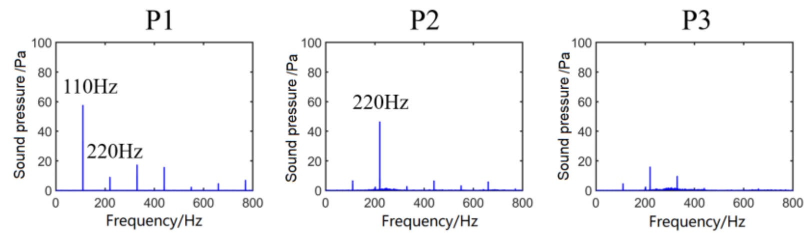

(a) 110Hz

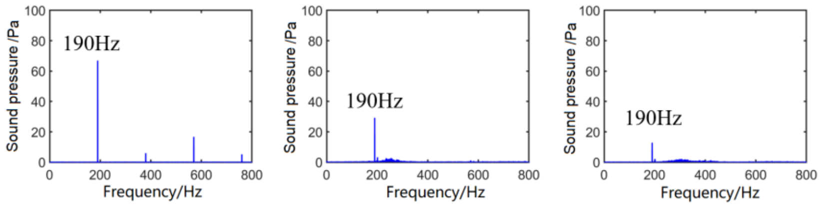

(b) 190Hz

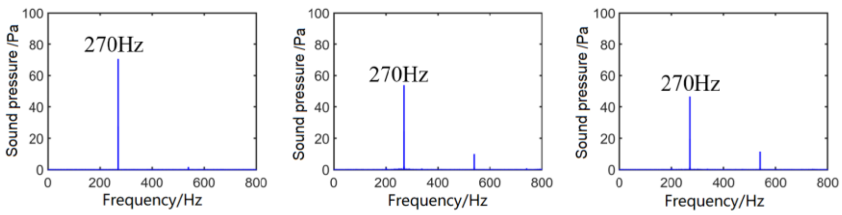

(c) 270Hz

Fig.3 Distribution of sound pressure fluctuation in combustion chamber

When acoustic excitation is added as 110 Hz to the inlet air, the combustion chamber tends to respond to frequency doubling, which shows to a certain extent that the oscillation of the axial staged combustion chamber may be more inclined to high-frequency oscillation. And the dominant frequency amplitude of the oscillation in the reburning zone is obviously lower than that in the main combustion zone, which may be caused by the significant difference between the acoustic excitation frequency and the natural frequency of the combustion chamber. Although the dominant frequency of oscillation in the reburning zone decreases, this decrease may result from the loss of sound pressure fluctuations in the downstream transmission process. As the acoustic excitation is 270 Hz, the sound pressure response in the combustion chamber is more pronounced. The sound pressure amplitude in the reburning zone only slightly decreases when the fluctuations are transmitted downstream, which shows that the oscillation in the reburning zone is enhanced.

3.2 Effect of forced combustion oscillation on reburning flame structure

From the analysis results of the sound pressure response in the combustion chamber with three acoustic excitation frequencies, it is indicated that the response in the reburning zone is the most obvious when the acoustic excitation frequency is 270 Hz, Therefore, this section selects the acoustic excitation frequency of 270 Hz to study the response characteristics of the reburning flame under the condition of combustion oscillation.

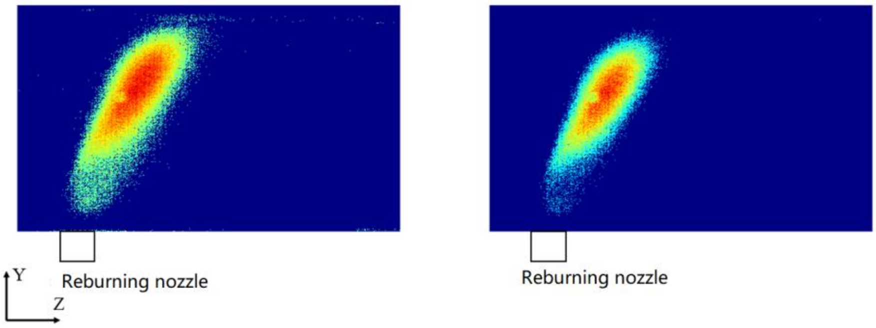

(a) Non-oscillation (b) Oscillation

Fig.4 Effect of combustion oscillation on the structure of reburning flame

To eliminate the interference of noise on the flame image, the gray value of the image less than 30% of the maximum in the flame photo is set to 0. Figure 4 shows the effect of combustion oscillations on the combustion flame structure. It shows that the combustion oscillation will lift the reburning flame compared with the stable combustion state. And this lifting effect may cause the flame to impinge on the upper wall more easily, narrowing the operating range of the combustion chamber. In addition, the combustion oscillation will also make the reburning flame to shrink toward the center of the flame. This shrinking may lead to an enhanced local heat release rate and consequently a local high-temperature hotspot, resulting in an increase in local NOx generation.

3.3 Effect of forced combustion oscillation on reburning flame position

During the processing of the reburning flame photos, 1000 transient images were selected for processing. The centroid of the reburning flame is extracted, which is defined as follows:

$$Mc = \left(\frac{\sum_{i=1}^{n} G_i\left(\frac{Z_i}{D}\right)}{\sum_{i=1}^{n} G_i}, \frac{\sum_{i=1}^{n} G_i\left(\frac{Y_i}{D}\right)}{\sum_{i=1}^{n} G_i}\right) \tag{3}$$

Where *Mc* is the centroid of the reburning flame, G_i is the gray value of the i^{th} pixel, Z_i/D and Y_i/D are the dimensionless coordinates of the i^{th} pixel in the Z direction and the Y direction, respectively.

Figure 5 plots the distribution of the centroid position of the transient reburning flame with and without combustion oscillations. It clearly shows that in the case of stable combustion, the centroid of the flame tends to fluctuate in the height direction (Z), and the fluctuation range in the Z direction is mainly distributed within Z/D=1.0~1.5. Comparatively, at the case of combustion oscillation, the centroid position of the reburning flame moves upward, mainly distributed around Y/D=4. And the band area of the centroid position fluctuation transforms from Z direction distribution to the Y direction distribution.

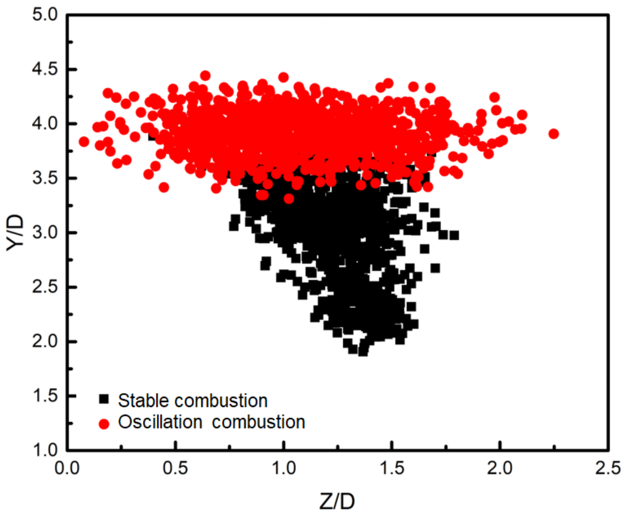

Fig.5 Distribution of centroid position of the transient reburning flame

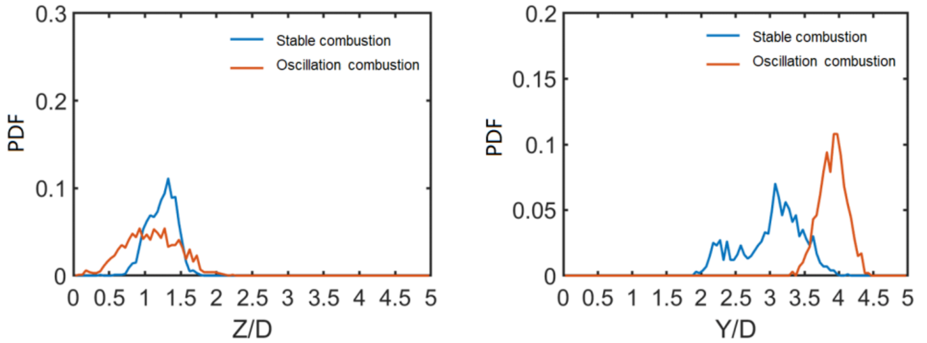

(a) Fluctuation of centroid in Z direction (b) Fluctuation of centroid in Y direction

Fig.6 Effect of combustion oscillation on the fluctuation of the flame centroid

In order to study the probability distribution of the fluctuation of the reburning flame centroid, we selected 0.05 D as the interval in the Z and the Y direction to describe the distribution probability of the reburning flame in each interval unit.

Figure 6 shows the effect of combustion oscillations on the fluctuation of the centroid position. It is implied that the combustion oscillation generally does not change the centroid position in the Z direction (maintained at about Z/D=1.2). But it will lift the average centroid position from Y/D=3.2 to Y/D= 4. In addition, the combustion oscillation will narrow the fluctuation range of the re-ignition flame in the Y direction but expand in the Z direction. The movement of the reburning flame in the Z direction will change the residence time of the high-temperature flue gas in the high-temperature area, which will consequently affect the NOx and CO emissions at the outlet of the combustion chamber. The changes in the range of fluctuations in the two directions indicate that when the inlet fluctuations are transmitted to the combustion chamber, the axial oscillations dominate. The fluctuations in other directions are limited by the walls of the combustion chamber during the transmission process. The fluctuations will collide with the walls and lose energy until they disappear completely.

Figure 7 shows the fast Fourier transform results of the centroid position fluctuation of the reburning flame in the Z direction, where z/D is the ratio of the fluctuation amplitude in the Z direction to the diameter of the reburning jet hole.

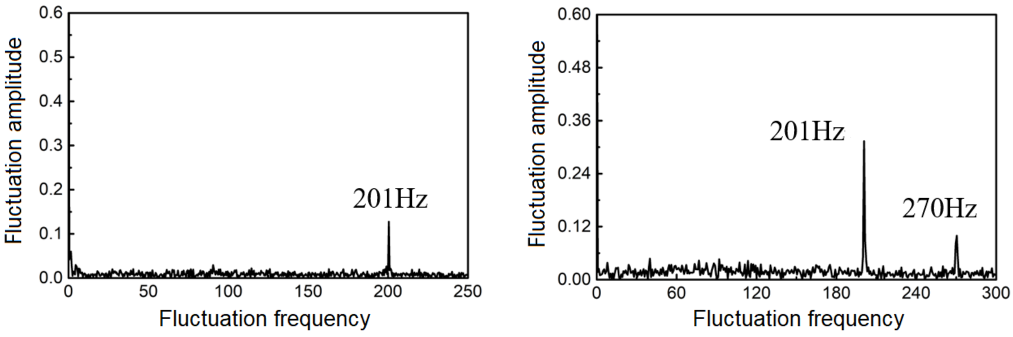

(a)Non-oscillation (b)Oscillation

Fig.7 Fast Fourier transform of fluctuation of the centroid position in the Z direction

It can be seen from Fig. 7(a) that the fluctuation frequency is 201 Hz along the Z direction in the case of stable combustion, which may be due to the disturbance of the reburning jet inlet or the flow field. In addition, the presence of the fluctuating dominant frequency did not cause combustion oscillations in the combustion chamber, which indicates that the periodic centroid fluctuations of the reburning flame may not necessarily be the cause of combustion oscillations. Fig. 7(b) demonstrates that the reburning flame is affected by the acoustic excitation at the oscillation case of oscillation. The centroid fluctuation presents a dominant frequency of 270 Hz. The generation of the dominant frequency suggests that the combustion of the reburning flame has a significant disturbance to the combustion chamber inlet, that is, the inlet disturbance will influence the stability of the reburning flame. Moreover, introducing acoustic excitation will also increase the amplitude of the original fluctuation of the reburning flame, which shows that the inlet fluctuation affects the flow field in the reburning zone. The reburning flame is affected, enhancing the original disturbance, and making the flame fluctuation more distinct.

Figure 8 shows the fast Fourier transform results of the centroid fluctuation of the reburning flame in the Y direction, where y/D is the ratio of the fluctuation amplitude in the Y direction to the diameter of the reburning jet hole.

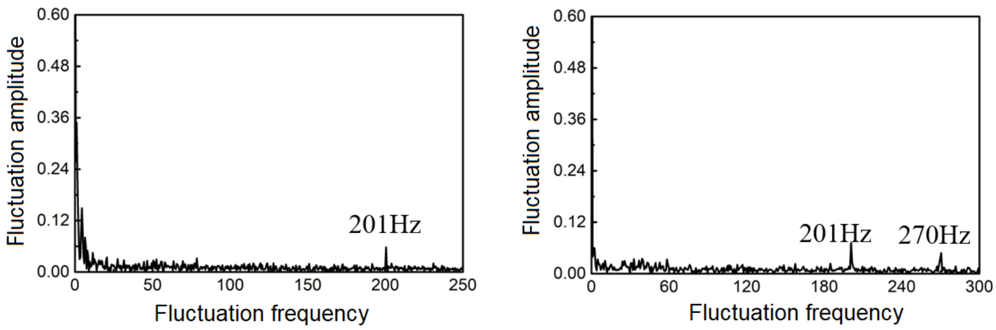

(a)Non-oscillation (b) Oscillation

Fig.8 Fast Fourier transform of fluctuation of the centroid position in the Y direction

4.Conclusion

In this work, disturbance is added to the main combustion air inlet by means of acoustic excitation, and the response of the sound pressure fluctuation in the combustion chamber and the characteristics of the reburning flame are in an axial staged combustor. The main conclusions are as follows:

(1) The main frequency of the oscillation in the combustion chamber is basically the same as the frequency of the acoustic excitation. When the acoustic excitation of 110 Hz is imposed to the main air inlet, the sound pressure response in the combustion chamber tends to double frequency. When the acoustic excitation is at the frequency of 190 Hz, the dominant frequency of the oscillation in the reburning zone reduces, which may be caused by the loss of sound pressure fluctuations in the downstream transmission process. As the excitation frequency is 270Hz, the sound pressure response in the combustion chamber is more obvious. And the sound pressure amplitude in the reburning zone is only slightly reduced during the fluctuations being transmitted downstream.

(2) Compared with the stable combustion, the combustion oscillation lifts the reburning flame (the average centroid position of the reburning flame in the height direction rises from Y/D=3.2 to Y/D=4). The reburning flame shrinks toward the flame center, and the band area where the flame centorid fluctuates is transformed from distribution in the height direction to the streamwise direction.

(3) The inlet fluctuations are transmitted to the combustion chamber, and the axial oscillation is dominant. Combustion oscillation will narrow the fluctuation range of the reburning flame in the Y direction but expand in the Z direction. In the case of non-oscillation, the dominant frequency (201 Hz) of the centroid fluctuation in the reburning flame appears along the Z and Y directions. And the dominant frequency amplitude of the oscillation in the Z direction is higher. In the case of oscillation, the centroid fluctuation generates a dominant frequency of 270 Hz along the Z and Y directions. The original fluctuation amplitude of the reburning flame in the Z direction increases, and there is no obvious change in the Y direction.

ACKNOWLEDGMENTS

This work is supported by National Science and Technology Major Project of China（J2019-III-0020-0064）.

References

[1] Winkler D, Geng W, Engelbrecht G, et al. Staged combustion concept for gas turbine[J]. Journal of the Global Power and Propulsion Society, 2017, 1: 184-194.
[2] Goh E, Sirignano M, Nair V, et al. Modeling of minimum NOx in staged-combustion architectures at elevated temperatures[C]// Proceedings of the ASME Turbo Expo 2017: Turbomachinery Technical Conference and Exposition. Volume 4A: Combustion, Fuels and Emissions. Charlotte, North Carolina, USA. June 26–30, 2017. V04AT04A048. ASME.
[3] Karim H, Natarajan J, Narra V, et al. Staged combustion system for improved emissions operability and flexibility for 7HA class heavy duty gas turbine engine[C]// Proceedings of the ASME Turbo Expo 2017: Turbomachinery Technical Conference and Exposition. Volume 4A: Combustion, Fuels and Emissions. Charlotte, North Carolina, USA. June 26–30, 2017. ASME.
[4] Romoser C E, Harper J, Wilson M B, et al. E-class late fuel staging technology delivers flexibility leap[C]// Proceedings of the ASME Turbo Expo 2016: Turbomachinery Technical Conference and Exposition. Volume 4B: Combustion, Fuels and Emissions. Seoul, South Korea. June 13–17, 2016. ASME.
[5] Tanaka R, Koji T, Ryu M, et al. Development of high efficient 30MW class gas turbine: The Kawasaki L30A[C]// Proceedings of the ASME Turbo Expo 2012: Turbine Technical Conference and Exposition. Volume 3: Cycle Innovations; Education; Electric Power; Fans and Blowers; Industrial and Cogeneration. Copenhagen, Denmark. June 11–15, 2012. pp. 883-889. ASME.
[6] Pennell D A, Bothien M R, Ciani A, et al. An introduction to the Ansaldo GT36 constant pressure sequential combustor[C]// Proceedings of the ASME Turbo Expo 2017: Turbomachinery Technical Conference and Exposition. Volume 4B: Combustion, Fuels and Emissions. Charlotte, North Carolina, USA. June 26–30, 2017. ASME.
[7] WANG Z. Study on axial staged premixed combustion characteristics of natural gas[D]. University of Chinese Academy of Sciences (Institute of Engineering Thermophysics, Chinese Academy of Sciences), 2019.
[8] Yi T A, Brh B, Jiang N A, et al. Autoignition-controlled flame initiation and flame stabilization in a reacting jet in crossflow[J]. Proceedings of the Combustion Institute, 2019, 37(2): 2109-2116.
[9] Roa M, Lamont W G, Meyer S E, et al. Emission measurements and OH-PLIF of reacting hydrogen jets in vitiated crossflow for stationary gas turbines[C]// Proceedings of the ASME Turbo Expo 2012: Turbine Technical Conference and Exposition. Volume 2: Combustion, Fuels and Emissions, Parts A and B. Copenhagen, Denmark. June 11–15, 2012. pp. 491-498. ASME.
[10] Zheng X. Study on pollutant emission and cross jet flame characteristics of fuel axial staged combustion[D]. University of Chinese Academy of Sciences (Institute of Engineering Thermophysics, Chinese Academy of Sciences), 2020.
[11] Ni A, Polifke W, Joos F. Ignition delay time modulation as a contribution to thermo-acoustic instability in sequential combustion[C]// Proceedings of the ASME Turbo Expo 2000: Power for Land, Sea, and Air. Volume 2: Coal, Biomass and Alternative Fuels; Combustion and Fuels; Oil and Gas Applications; Cycle Innovations. Munich, Germany. May 8–11, 2000. ASME.
[12] Schulz O, Doll U, Ebi D, et al. Thermoacoustic instability in a sequential combustor: Large eddy simulation and experiments[J]. Proceedings of the Combustion Institute, 2019, 37(4): 5325-5332.